ENHANCEMENTS OF UNITARY ESPRIT FOR NON-CIRCULAR SOURCES

Martin Haardt and Florian Römer

Ilmenau University of Technology, Communications Research Laboratory
P.O. Box 100565, D-98684 Ilmenau, Germany
martin.haardt@tu-ilmenau.de, florian.roemer@gmx.de

ABSTRACT

Subspace based high-resolution parameter estimation algorithms often use forward-backward averaging to enhance their resolution, especially in case of correlated sources. Further enhancements can be achieved if the source signals are non-circular. In this paper, we derive an efficient subspace estimation scheme that exploits the non-circularity of the sources and already includes forward-backward averaging. Moreover, appropriate spatial smoothing techniques are introduced. Completely real-valued implementations of *1-D* and *2-D Unitary ESPRIT for non-circular sources* are presented as examples. In these cases, *NC Unitary ESPRIT* improves the resolution capability and the noise robustness of *standard ESPRIT* as well as *Unitary ESPRIT* and can handle more sources than sensors.

1. INTRODUCTION

Estimating the directions of arrival of several wavefronts impinging on an array of sensors is a requirement in a variety of applications including radar, mobile communications, sonar, and seismology. Subspace based high-resolution parameter estimation schemes like ESPRIT and MUSIC have become very popular.

Forward-backward averaging is a preprocessing procedure for subspace based parameter estimation schemes that is employed in many signal processing applications such as direction finding [1], beamforming [2], spectral estimation [3], and speech processing. It effectively doubles the number of available observations and decorrelates two highly correlated wavefronts without sacrificing aperture. In the array processing context, it is applicable to *centro-symmetric* array configurations [4]. The computational complexity of any direction finding method implemented with forward-backward averaging can be reduced significantly. This reduction is achieved by constructing invertible transformations that map centro-Hermitian matrices to real matrices [5]. These results were used to transform the complex covariance matrix of centro-symmetric arrays into a real matrix of the same size [6] to reduce the computational load of adaptive beamforming schemes [2]. The computational complexity is reduced below that of an analogous forward only implementation [7]. Thus, effectively twice the amount of data is processed with less computations [8].

Many modern telecommunication systems or satellite systems deal with non-circular sources, where amplitude modulated (AM) or BPSK modulated signals are often employed.[1] Improved versions of ESPRIT, spectral MUSIC, and Root-MUSIC that exploit the non-circularity of the sources have been proposed in [9, 10], [11], and [12], respectively.

In this paper, we present an efficient square-root (direct data) implementation of subspace based techniques for non-circular sources that incorporates forward-backward averaging and (optionally) also spatial smoothing techniques. Completely real-valued implementations of 1-D and 2-D Unitary ESPRIT for non-circular sources (*NC Unitary ESPRIT*) will be presented as examples. Multidimensional extensions of *NC Unitary ESPRIT* to more than two dimensions are straightforward [13].

2. DATA MODEL

Assume that the emitting sources are narrow-band and in the far field, so that the d wavefronts impinging on the array are planar. Using a centro-symmetric antenna array of M sensors, the array measurements will be collected in the matrix

$$\boldsymbol{X} = \boldsymbol{A}\boldsymbol{S} + \boldsymbol{N} \in \mathbb{C}^{M \times N}, \tag{1}$$

where the $\boldsymbol{S} \in \mathbb{C}^{d \times N}$ contains N subsequent snapshots from each of the d sources, $\boldsymbol{N} \in \mathbb{C}^{M \times N}$ represents the additive noise at each of the M antenna elements taken from a zero mean random process with covariance matrix $\sigma_N^2 \boldsymbol{I}_M$, and $\boldsymbol{A} \in \mathbb{C}^{M \times d}$ is the array steering matrix consisting of the d array steering vectors $\boldsymbol{a}(\mu_i)$.

Due to the non-circularity of the sources, the signals impinging on the array can be expressed as

$$\boldsymbol{S} = \boldsymbol{\Psi}\boldsymbol{S}_0, \quad \text{where} \quad \boldsymbol{S}_0 \in \mathbb{R}^{d \times N} \tag{2}$$

and the diagonal matrix $\boldsymbol{\Psi} = \operatorname{diag}\left\{e^{\mathrm{j}\varphi_i}\right\}_{i=1}^{d}$ contains arbitrary complex phase shifts that can be different for each signal. Note that in the single snapshot case ($N = 1$), the non-circularity condition (2) does not represent any restriction.

3. SUBSPACE ESTIMATION FOR NON-CIRCULAR SOURCES

Since *Unitary ESPRIT* involves forward-backward averaging, it can efficiently be formulated in terms of real-valued computations throughout [8] due to a bijective mapping between centro-Hermitian and real matrices [5]. To this end, let us define left $\boldsymbol{\Pi}$-real matrices [5, 8], i.e., matrices $\boldsymbol{Q} \in \mathbb{C}^{p \times q}$ satisfying

F. Römer is currently on leave at McMaster University, Hamilton, Ontario, Canada.

[1] A signal is called non circular if its amplitudes lie on a line in the complex I-Q-diagram, e.g., BPSK, ASK, AM, or PAM-modulated signals.

$\mathbf{\Pi}_p \boldsymbol{Q}^* = \boldsymbol{Q}$. $\mathbf{\Pi}_M$ is the $M \times M$ exchange matrix with ones on its antidiagonal and zeros elsewhere. The unitary matrix

$$\boldsymbol{Q}_{2n+1} = \frac{1}{\sqrt{2}} \begin{bmatrix} \boldsymbol{I}_n & \boldsymbol{0} & \mathrm{j}\,\boldsymbol{I}_n \\ \boldsymbol{0}^T & \sqrt{2} & \boldsymbol{0}^T \\ \mathbf{\Pi}_n & \boldsymbol{0} & -\mathrm{j}\,\mathbf{\Pi}_n \end{bmatrix}, \tag{3}$$

for example, is left $\mathbf{\Pi}$-real of odd order. A unitary left $\mathbf{\Pi}$-real matrix of size $2n \times 2n$ is obtained from (3) by dropping its center row and center column. More left $\mathbf{\Pi}$-real matrices can be constructed by post-multiplying a left $\mathbf{\Pi}$-real matrix $\boldsymbol{Q}$ by an arbitrary real matrix $\boldsymbol{R}$, i.e., every matrix $\boldsymbol{Q}\,\boldsymbol{R}$ is left $\mathbf{\Pi}$-real.

A centro-Hermitian square-root factor of the forward-backward averaged covariance matrix is given by

$$\boldsymbol{Z} = \begin{bmatrix} \boldsymbol{X} & \mathbf{\Pi}_M\,\boldsymbol{X}^*\,\mathbf{\Pi}_N \end{bmatrix} \in \mathbb{C}^{M \times 2N}. \tag{4}$$

Therefore, $\varphi(\boldsymbol{Z}) = \boldsymbol{Q}_M^H\,\boldsymbol{Z}\boldsymbol{Q}_{2N}$ is a real-valued matrix.

If the source signals are non-circular, we can "double" the number of available sensors by defining

$$\boldsymbol{X}^{(\mathrm{nc})} = \begin{bmatrix} \boldsymbol{X} \\ \mathbf{\Pi}_M\,\boldsymbol{X}^* \end{bmatrix} \in \mathbb{C}^{2M \times N} \tag{5}$$

that admits a factorization

$$\begin{aligned} \boldsymbol{X}^{(\mathrm{nc})} &= \begin{bmatrix} \boldsymbol{A}\,\boldsymbol{S} \\ \mathbf{\Pi}\,\boldsymbol{A}^*\,\mathbf{\Psi}^*\,\boldsymbol{S}_0 \end{bmatrix} + \begin{bmatrix} \boldsymbol{N} \\ \mathbf{\Pi}\,\boldsymbol{N}^* \end{bmatrix} \\ &= \underbrace{\begin{bmatrix} \boldsymbol{A} \\ \mathbf{\Pi}\,\boldsymbol{A}^*\,\mathbf{\Psi}^*\,\mathbf{\Psi}^{-1} \end{bmatrix}}_{\boldsymbol{A}^{(\mathrm{nc})}} \boldsymbol{S} + \underbrace{\begin{bmatrix} \boldsymbol{N} \\ \mathbf{\Pi}\,\boldsymbol{N}^* \end{bmatrix}}_{\boldsymbol{N}^{(\mathrm{nc})}} \end{aligned}$$

similar to (1). Since the new array steering matrix $\boldsymbol{A}^{(\mathrm{nc})}$ is of size $2M \times N$, we have virtually doubled the number of antennas, which yields in a better resolution and a higher number of separable sources.

In analogy to (4), let us define:

$$\begin{aligned} \boldsymbol{Z}^{(\mathrm{nc})} &= \begin{bmatrix} \boldsymbol{X}^{(\mathrm{nc})} & \mathbf{\Pi}_{2M}\,\boldsymbol{X}^{(\mathrm{nc})*}\,\mathbf{\Pi}_N \end{bmatrix} \\ &= \begin{bmatrix} \boldsymbol{X} & \boldsymbol{X}\,\mathbf{\Pi}_N \\ \mathbf{\Pi}_M\,\boldsymbol{X}^* & \mathbf{\Pi}_M\,\boldsymbol{X}^*\,\mathbf{\Pi}_N \end{bmatrix} \in \mathbb{C}^{2M \times 2N}. \end{aligned} \tag{6}$$

Note, however, that $\boldsymbol{Z}^{(\mathrm{nc})}\,\boldsymbol{Z}^{(\mathrm{nc})H} = 2 \cdot \boldsymbol{X}^{(\mathrm{nc})}\,\boldsymbol{X}^{(\mathrm{nc})H}$. Therefore, both matrices contain the same column spaces. Consequently, $\boldsymbol{X}^{(\mathrm{nc})}$ as defined in equation (5) already includes forward-backward-averaging.

Due to the fact that $\boldsymbol{Z}^{(\mathrm{nc})}$ is centro-Hermitian, it can be transformed into a real valued matrix according to [14]

$$\varphi(\boldsymbol{Z}^{(\mathrm{nc})}) = \boldsymbol{Q}_{2M}^H\,\boldsymbol{Z}^{(\mathrm{nc})}\boldsymbol{Q}_{2N} = 2 \begin{bmatrix} \mathrm{Re}\{\boldsymbol{X}\} & \boldsymbol{0}_{M \times N} \\ \mathrm{Im}\{\boldsymbol{X}\} & \boldsymbol{0}_{M \times N} \end{bmatrix}. \tag{7}$$

4. 1-D UNITARY ESPRIT FOR NON-CIRCULAR SOURCES

In this section, we will restrict our discussion to 1-D uniform linear (equispaced) sensor arrays (ULAs) consisting of M identical antennas. Then the array steering vectors are given by

$$\mathbf{a}(\mu_i) = \begin{bmatrix} 1 & e^{\mathrm{j}\mu_i} & e^{\mathrm{j}2\mu_i} & \cdots & e^{\mathrm{j}(M-1)\mu_i} \end{bmatrix}^T, \tag{8}$$

$1 \le i \le d$, where $\mu_i = \frac{2\pi}{\lambda}\Delta \sin\theta_i$. Here, Δ denotes the spacing between adjacent sensors, λ the common wavelength of the incident wavefronts, and θ_i the direction of arrival (DOA) of the i-th wavefront.

The d dominant left singular vectors $\boldsymbol{E}_s \in \mathbb{R}^{2M \times d}$ of $\varphi(\boldsymbol{Z}^{(\mathrm{nc})})$ can be obtained through a real-valued SVD of (7). The zero columns and the scaling factor can, of course, be dropped as they are not required to determine the dominant subspace of $\varphi(\boldsymbol{Z}^{(\mathrm{nc})})$. In case of a ULA with maximum overlap, the selection matrices for standard ESPRIT are defined as

$$\mathbf{J}_1 = \begin{bmatrix} \mathbf{I}_{M-1} & \mathbf{0}_{(M-1)\times 1} \end{bmatrix} \text{ and } \mathbf{J}_2 = \begin{bmatrix} \mathbf{0}_{(M-1)\times 1} & \mathbf{I}_{M-1} \end{bmatrix}.$$

If the sources are non-circular, these selection matrices should be modified in the following fashion,

$$\boldsymbol{J}_k^{(\mathrm{nc})} = \begin{bmatrix} 1 & 0 \\ 0 & 1 \end{bmatrix} \otimes \boldsymbol{J}_k \in \mathbb{R}^{2m \times 2M}, \quad k = 1, 2 \tag{9}$$

where $\otimes$ denotes the Kronecker product and $m = M - 1$. For *NC Unitary ESPRIT* they are transformed as

$$\begin{aligned} \mathbf{K}_1^{(\mathrm{nc})} &= 2 \cdot \mathrm{Re}\left\{ \mathbf{Q}_{2m}^H \mathbf{J}_2^{(\mathrm{nc})} \mathbf{Q}_{2M} \right\} \text{ and} \\ \mathbf{K}_2^{(\mathrm{nc})} &= 2 \cdot \mathrm{Im}\left\{ \mathbf{Q}_{2m}^H \mathbf{J}_2^{(\mathrm{nc})} \mathbf{Q}_{2M} \right\}. \end{aligned} \tag{10}$$

Then, the overdetermined *real-valued* set of equations

$$\boldsymbol{K}_1^{(\mathrm{nc})} \boldsymbol{E}_s \mathbf{\Upsilon} \approx \boldsymbol{K}_2^{(\mathrm{nc})} \boldsymbol{E}_s \tag{11}$$

can, for instance be solved via least squares (LS) [8]. Finally, the spatial frequencies μ_i are estimated as $\mu_i = 2\arctan(\omega_i)$ from the real-valued eigenvalues ω_i of $\mathbf{\Upsilon}$. If all eigenvalues ω_i of the estimated $\mathbf{\Upsilon}$ are real, they provide a reliable estimate [8]. Otherwise, i.e., if some of the eigenvalues ω_i occur in complex conjugate pairs, the *Unitary ESPRIT reliability test* has "failed", and the algorithm has to be restarted with more or more reliable measurements.

To be able to separate more than two coherent wavefronts, we combine spatial smoothing techniques [1] with the *Unitary ESPRIT* concept. Spatial smoothing is a preprocessing scheme that divides the array of M sensors into L subarrays, each containing $M_{\mathrm{sub}} = M - L + 1$ sensor elements. Let the selection matrix that corresponds to the ℓth subarray be defined as

$$\mathbf{J}_\ell^{(M)} = \begin{bmatrix} \mathbf{0}_{M_{\mathrm{sub}} \times (\ell-1)} & \mathbf{I}_{M_{\mathrm{sub}}} & \mathbf{0}_{M_{\mathrm{sub}} \times (L-\ell)} \end{bmatrix}, \tag{12}$$

$1 \le \ell \le L$. In case of *NC Unitary ESPRIT*, spatial smoothing cannot be performed on $\boldsymbol{X}$ before $\boldsymbol{X}^{(\mathrm{nc})}$ is formed according to (5) as it would destroy the special structure of the source signals. Instead, we have to apply a modified smoothing concept directly to $\boldsymbol{X}^{(\mathrm{nc})}$ by selecting $2M_{\mathrm{sub}}$ out of $2M$ virtual sensors. Hence, the selection matrices (12) are extended to yield

$$\mathbf{J}_\ell^{(M,\mathrm{nc})} = \begin{bmatrix} 1 & 0 \\ 0 & 1 \end{bmatrix} \otimes \boldsymbol{J}_\ell^{(M)} \in \mathbb{R}^{2M_{\mathrm{sub}} \times 2M}. \tag{13}$$

The resulting "spatially smoothed" data matrix

$$\boldsymbol{X}_{\mathrm{SS}}^{(\mathrm{nc})} = \begin{bmatrix} \boldsymbol{J}_1^{(M,\mathrm{nc})}\boldsymbol{X}^{(\mathrm{nc})} & \boldsymbol{J}_2^{(M,\mathrm{nc})}\boldsymbol{X}^{(\mathrm{nc})} & \cdots & \boldsymbol{J}_L^{(M,\mathrm{nc})}\boldsymbol{X}^{(\mathrm{nc})} \end{bmatrix}$$

is of size $2M_{\mathrm{sub}} \times NL$ and replaces the data matrix $\boldsymbol{X}^{(\mathrm{nc})}$ in (6) if spatial smoothing is incorporated into the *NC Unitary ESPRIT*

[1] It can easily be shown that $\boldsymbol{N}^{(nc)}$ has the same statistical properties as $\boldsymbol{N}$.

concept. Note that the resulting $\varphi(\boldsymbol{Z}_{\mathrm{SS}}^{(\mathrm{nc})}) = \boldsymbol{Q}_{2M}^H \boldsymbol{Z}_{\mathrm{SS}}^{(\mathrm{nc})} \boldsymbol{Q}_{2NL}$ is again real-valued and can efficiently be obtained from $\boldsymbol{X}$.

As mentioned before, *NC Unitary ESPRIT* allows us to resolve more source signals. If none of the sources is highly correlated with another source, *NC Unitary ESPRIT* can handle up to $\min\{2(M-1), N\}$ sources (as compared to $\min\{M-1, 2N\}$ sources in case of Unitary ESPRIT). Spatial smoothing can be applied to increase the rank if the number of snapshots N is limited. If the sources are highly correlated, spatial smoothing is needed for decorrelation. The more subarrays we use, the more sources we can decorrelate, but the less sensor elements per subarray are left. Hence, for d coherent sources, the following limitations apply:

Unitary ESPRIT	NC Unitary ESPRIT
$L_{\min} = \lceil \frac{d}{2} \rceil$	$L_{\min} = d$
$L_{\max} = M - d$	$L_{\max} = \lfloor M - \frac{d}{2} \rfloor$
$\rightarrow d_{\max} = \lfloor \frac{2}{3} M \rfloor$	$\rightarrow d_{\max} = \lfloor \frac{2}{3} M \rfloor$

Yet, it is important to note that the robustness of the estimation decreases severely with the number of source signals, i.e., a very high SNR is needed for a reliable estimation.

5. 2-D UNITARY ESPRIT FOR NON-CIRCULAR SOURCES

Extensions of *NC Unitary ESPRIT* to the multidimensional case are straightforward if the modifications discussed for *1-D Unitary ESPRIT* in the previous section are applied to *R-D Unitary ESPRIT* for $R \geq 2$ as presented in [13].

As an example, consider the 2-D case. Let us focus our attention on uniform rectangular arrays (URAs) consisting of $M = M_\mu \times M_\nu$ sensor elements. The 2-D spatial frequencies of the d impinging wavefronts wih respect to the x- and y-axis are given by

$$\mu_i = \frac{2\pi}{\lambda} \Delta_x \cos\phi_i \sin\theta_i \quad \text{and} \quad \nu_i = \frac{2\pi}{\lambda} \Delta_y \sin\phi_i \sin\theta_i,$$

respectively. Here, ϕ_i and θ_i, $1 \leq i \leq d$, denote the azimuth and elevation angles, λ is the wavelength, and Δ_x as well as Δ_y are the sensor distances in x- and y-direction.

Without spatial smoothing the number of resolvable sources for *2-D NC Unitary ESPRIT* is equal to

$$d_{\max} = \min\{2(M_\mu - 1)M_\nu, 2(M_\nu - 1)M_\mu, N\}$$

(as compared to $d_{\max} = \min\{(M_\mu - 1)M_\nu, (M_\nu - 1)M_\mu, 2N\}$ for *2-D Unitary ESPRIT*). If all the d sources are coherent and spatial smoothing with L_μ subarrays in x-direction and L_ν subarrays in y-direction is used, these inequalities have to hold:

$$\begin{aligned} d &\leq L_\mu L_\nu \\ d &\leq 2 \cdot \min\{(M_\mu - L_\mu)(M_\nu - L_\nu + 1), \\ &\quad (M_\nu - L_\nu)(M_\mu - L_\mu + 1)\} \end{aligned} \tag{14}$$

for *2-D NC Unitary ESPRIT* and

$$\begin{aligned} d &\leq 2 \cdot L_\mu L_\nu \\ d &\leq \min\{(M_\mu - L_\mu)(M_\nu - L_\nu + 1), \\ &\quad (M_\nu - L_\nu)(M_\mu - L_\mu + 1)\} \end{aligned} \tag{15}$$

for *2-D Unitary ESPRIT*. For both algorithms $d_{\max} = \lfloor (M_\mu M_\nu)/3 \rfloor$ is a lower bound as well as a good approximation for the number sources that are actually resolvable.

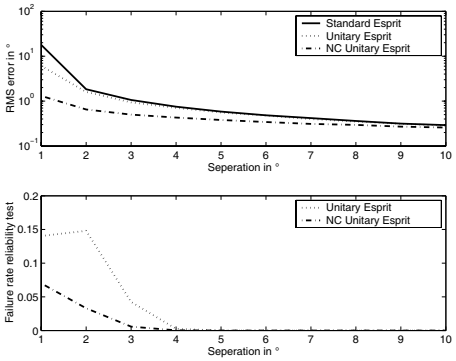

Fig. 1. RMS error of the estimated DOAs as a function of the separation in the 1-D case ($M = 10$ sensors, $N = 20$, SNR = 10 dB, 4000 trial runs)

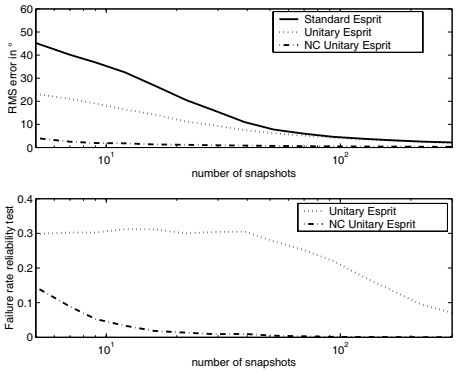

Fig. 2. RMS error of the estimated DOAs as a function of the number of snapshots N in the 1-D case ($M = 6$ sensors, $\theta_1 = 0°$, $\theta_2 = 5°$, $\theta_3 = 10°$, SNR = 15 dB, 4000 trial runs)

6. SIMULATION RESULTS

In this section, we present some simulation results to illustrate the performance of *1-D* and *2-D NC Unitary ESPRIT*. First, we consider a ULA with $M = 10$ elements and a window length of $N = 20$ snapshots. Two 4-ASK signals with SNRs of 10 dB impinge on the array from $\theta_1 = -(\frac{\mathrm{sep}}{2})°$ and $\theta_2 = (\frac{\mathrm{sep}}{2})°$. Fig. 1 depicts the RMS error of the estimated DOAs as a function of the separation of the sources as well as the failure rate of the reliability test for both versions of *Unitary ESPRIT*. Especially for small separations, *NC Unitary ESPRIT* performs significantly better than the other algorithms. Fig. 2 depicts the performance for three sources located at $\theta_1 = 0°$, $\theta_2 = 5°$, and $\theta_3 = 10°$ as a function of the number of snapshots N. Fig. 3 shows the RMS error of the estimated DOA of source 1 as the number of sources d is varied from 1 to 10. Note that $\theta_1 = 0°$, whereas the additional sources are separated by $15°$.

Fig. 4 depicts a similar scenario in the 2-D case. A URA consisting of 3×3 elements collects 20 snapshots of the d sources with an SNR of 30 dB and a separation of 0.2 (in μ and ν), the RMS error of the first source in the μ-ν-plane (that is fixed at $[\mu_1, \nu_1] = [0, 0]$) is averaged over 1000 trials.

Next, Fig. 5 shows the RMS error of the estimated spatial frequencies in the μ-ν-plane as a function of the separation between the two sources located at $[\mu_1, \nu_1] = [-\mathrm{sep}/2, 0]$ and $[\mu_2, \nu_2] = [\mathrm{sep}/2, \mathrm{sep}]$. Finally, Fig. 6 depicts the RMS error of the estimated

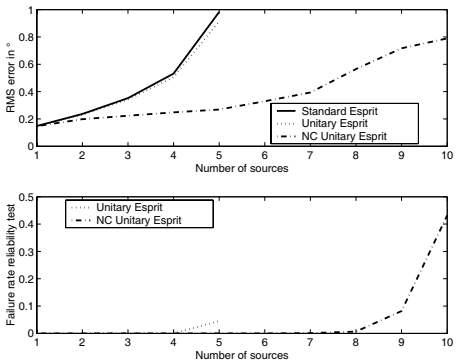

Fig. 3. RMS error of the estimated DOA of source 1 as a function of the number of sources d in the 1-D case ($M = 6$ sensors, $\theta_1 = 0^\circ$, source separation 15°, $N = 20$, SNR = 15 dB, 5000 trial runs)

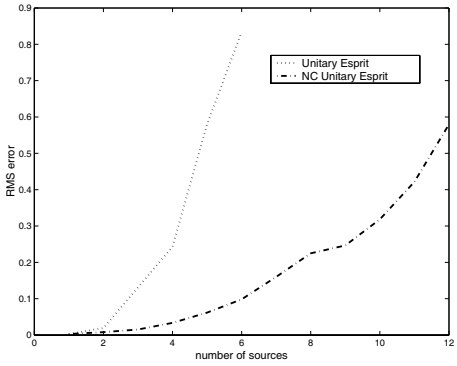

Fig. 4. RMS error of the estimated spatial frequencies of source 1 as a function of the number of sources d in the 2-D case (3×3 sensors, $[\mu_1, \nu_1] = [0, 0]$, source separation 0.3, $N = 20$, SNR = 30 dB, 5000 trial runs)

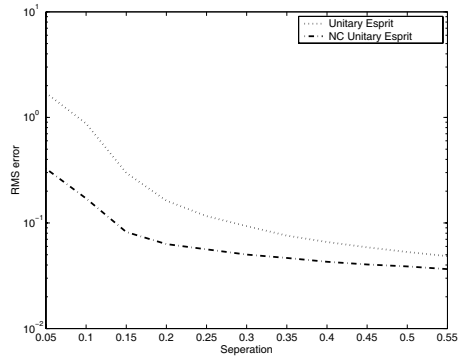

Fig. 5. RMS error of the estimated spatial frequencies as a function of the separation between the two sources located at $[\mu_1, \nu_1] = [-\mathrm{sep}/2, 0]$ and $[\mu_2, \nu_2] = [\mathrm{sep}/2, \mathrm{sep}]$ in the 2-D case (4×4 sensors, $N = 20$, SNR = 10 dB, 4000 trial runs)

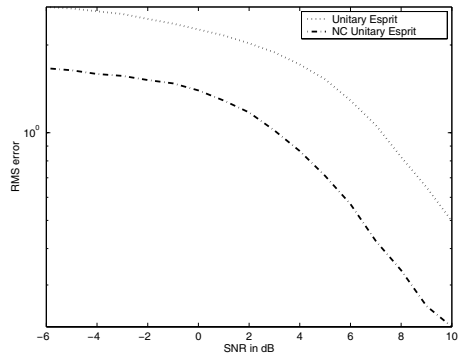

Fig. 6. RMS error of the estimated spatial frequencies as a function of the SNR in the 2-D case (4×4 sensors, $[\mu_1, \nu_1] = [0, 0]$, $[\mu_2, \nu_2] = [0, 0.25]$, $[\mu_3, \nu_3] = [0.25, 0]$, $N = 20$, 4000 trial runs)

spatial frequencies in the μ-ν-plane as a function of the SNR. The three sources are located at $[\mu_1, \nu_1] = [0, 0]$, $[\mu_2, \nu_2] = [0, 0.25]$, and $[\mu_3, \nu_3] = [0.25, 0]$.

7. CONCLUSIONS

Enhancements and efficient implementations of *Unitary ESPRIT* for non-circular source signals (such as BPSK, ASK, AM, or PAM) have been presented in this paper. Due to the fact that the number of available sensors is "virtually doubled," *NC Unitary ESPRIT* improves the resolution capability and the noise robustness of *standard ESPRIT* as well as *Unitary ESPRIT* and can handle more sources than sensors.

8. REFERENCES

[1] S. U. Pillai and B. H. Kwon, "Forward / backward spatial smoothing techniques for coherent signal identification," *IEEE Trans. Acoustics, Speech, and Signal Processing*, vol. ASSP-37, pp. 8–15, Jan. 1989.

[2] K. C. Huarng and C. C. Yeh, "Adaptive beamforming with conjugate symmetric weights," *IEEE Trans. Antennas and Propagation*, vol. 39, pp. 926–932, July 1991.

[3] R. Kumaresan and D. W. Tufts, "Estimating the parameters of exponentially damped sinusoids and pole-zero modeling in noise," *IEEE Trans. Acoustics, Speech, and Signal Processing*, vol. ASSP-30, pp. 833–840, Dec. 1982.

[4] G. Xu, R. H. Roy, and T. Kailath, "Detection of number of sources via exploitation of centro-symmetry property," *IEEE Trans. Signal Processing*, vol. 42, pp. 102–112, Jan. 1994.

[5] A. Lee, "Centrohermitian and skew-centrohermitian matrices," *Linear Algebra and its Applications*, vol. 29, pp. 205–210, 1980.

[6] K. C. Huarng and C. C. Yeh, "A unitary transformation method for angle-of-arrival estimation," *IEEE Trans. Signal Processing*, vol. 39, pp. 975–977, Apr. 1991.

[7] D. A. Linebarger, R. D. DeGroat, and E. M. Dowling, "Efficient direction finding methods employing forward / backward averaging," *IEEE Trans. Signal Processing*, vol. 42, pp. 2136–2145, Aug. 1994.

[8] M. Haardt and J. A. Nossek, "Unitary ESPRIT: How to obtain increased estimation accuracy with a reduced computational burden," *IEEE Trans. Signal Processing*, vol. 43, pp. 1232–1242, May 1995.

[9] M. Haardt and M. E. Ali-Hackl, "Unitary ESPRIT: How to exploit additional information inherent in the rotational invariance structure," in *Proc. IEEE Int. Conf. Acoust., Speech, and Signal Processing (ICASSP)*, Adelaide, Australia, Apr. 1994, vol. IV, pp. 229–232.

[10] A. Zoubir, P. Chargé, and Y. Wang, "Non circular sources localization with ESPRIT," in *Proc. European Conference on Wireless Technology (ECWT 2003)*, Munich, Germany, Oct. 2003.

[11] J. Galy, *Antenne adaptative: Du seconde ordre aux ordres supérieurs, applications aux signaux de télécommunications*, Ph.D. thesis, Toulouse, France, 1998.

[12] P. Chargé, Y. Wang, and J. Saillard, "A non circular sources direction finding method using polynomial rooting," *Signal Processing*, no. 81, pp. 1765–1770, 2001, Elsevier Science Publishers.

[13] M. Haardt and J. A. Nossek, "Simultaneous Schur decomposition of several non-symmetric matrices to achieve automatic pairing in multidimensional harmonic retrieval problems," *IEEE Trans. Signal Processing*, vol. 46, pp. 161–169, Jan. 1998.

[14] M. Haardt, *Efficient One-, Two-, and Multidimensional High-Resolution Array Signal Processing*, Shaker Verlag, Aachen, Germany, 1996, ISBN 3-8265-2220-6.